

Steric Hindrance-Induced Dual Fluorescence of Congested Benzenehexacarboxylates<sup>1</sup>Noritsugu Yamasaki,<sup>†</sup> Yoshihisa Inoue,<sup>\*,†</sup> Taizo Yokoyama,<sup>†</sup> Akira Tai,<sup>†</sup> Akito Ishida,<sup>‡</sup> and Setsuo Takamuku<sup>†</sup>*Contribution from the Department of Material Science, Faculty of Science, Himeji Institute of Technology, 2167 Shosha, Himeji, Hyogo 671-22, Japan, and the Institute of Scientific and Industrial Research, Osaka University, Mihogaoka, Ibaraki, Osaka 566, Japan.**Received July 30, 1990. Revised Manuscript Received October 19, 1990*

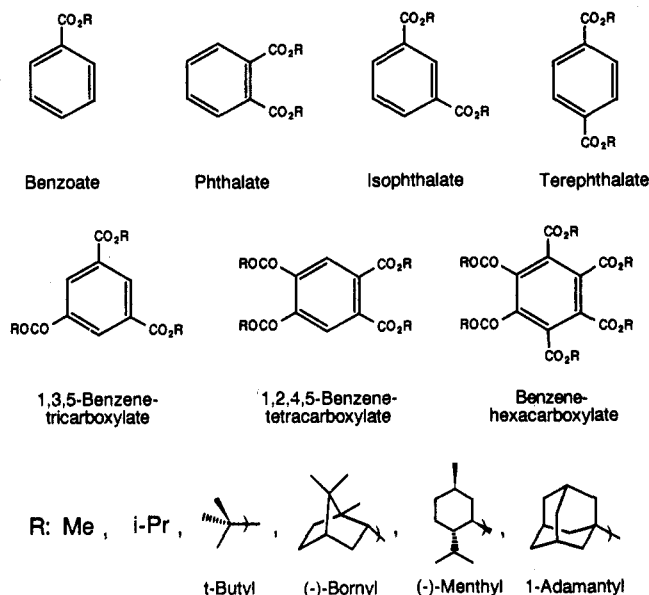
**Abstract:** Alkyl benzenetetra- and benzenehexacarboxylates were shown to fluoresce weakly in fluid solutions, in sharp contrast to entirely nonfluorescent mono-, di-, or tricarboxylates. Interestingly, benzenehexacarboxylates with bulky alkyl groups provide a novel dual-fluorescing molecular system involving a mechanism differing from the well-documented excimer formation, protonation/deprotonation, or twisted intramolecular charge transfer. Thus hexacarboxylates of isopropyl, *tert*-butyl, (-)-bornyl, (-)-menthyl, and 1-adamantyl alcohols show unambiguous, bulkiness-dependent dual fluorescence peaks with both small and substantially large Stokes shifts at room and/or low temperatures, whereas the hexamethyl ester and the corresponding tetracarboxylates with bulky alkyl groups never show such unusual fluorescence behavior. This dual fluorescence phenomenon is attributed to the decelerated conformational relaxation in the excited state owing to steric hindrance between adjacent bulky alkyl groups.

A wide variety of compounds and molecular systems are known to display dual fluorescence behavior in vapor<sup>2-6</sup> and solution phases.<sup>7-34</sup> Apart from the low-pressure experiments in the vapor phase, where the collisional deactivations of excited states are scarce, several distinctly different mechanisms have been proposed to rationalize the dual fluorescence phenomena in fluid solutions. The dual-fluorescing systems may be classified into the following categories according to the mechanism involved: (1) excited-state protonation/deprotonation<sup>7-11</sup> or proton transfer,<sup>12-17</sup> (2) intra- and intermolecular excimer/exciple formation,<sup>17-21</sup> (3) independent excitation of ground-state conformers,<sup>22</sup> (4) thermal population to a closely lying upper excited state,<sup>23</sup> (5) intramolecular charge-transfer emission of organosilanes,<sup>24,25</sup> and (6) twisted intramolecular charge transfer (TICT) involving rotation around single<sup>26-31</sup> or double bonds<sup>32-35</sup> in the excited state. In the last case, which might be related in a sense to the present system, the intramolecular charge transfer in an initially formed Franck-Condon (FC) state leads to charge separation especially in polar solvents, relaxing into a twisted excited state. Some energetic barrier between the initial FC and relaxed TICT states allows one to observe the dual fluorescence behavior in fluid solutions.

Unsubstituted benzenecarboxylates like alkyl benzoate are generally nonfluorescent in fluid solutions at room temperature, although, in low-temperature rigid matrices, weak fluorescence has been detected along with fairly intense phosphorescence at longer wavelengths.<sup>36-41</sup> The weak fluorescence in fluid solutions has been attributed to the rapid intersystem crossing to an  $n, \pi^*$  triplet state, which is located close in energy to the lowest excited  $\pi, \pi^*$  singlet state.<sup>36</sup> Nuclear substitution of benzoate with a highly electron-donating group, such as hydroxyl or amino, is known to enhance the fluorescence quantum yield dramatically.<sup>36,42</sup> On the contrary, electron-withdrawing groups have been believed to be ineffective in increasing the fluorescence quantum yield,<sup>36</sup> hence the photophysical behavior of benzenepolycarbonates has not been investigated extensively.

In the course of our study to effect highly stereodifferentiating asymmetric *Z-E* photoisomerization of cyclooctene sensitized by several chiral aromatic esters via singlet exciplexes,<sup>43</sup> we synthesized a series of novel benzenepolycarboxylates of bulky chiral alcohols like (-)-menthol and (-)-borneol as singlet photosensitizers for higher optical yields. Contrary to the anticipation mentioned above, the tetra- and hexasubstitutions with electron-withdrawing alkoxy carbonyl groups rather enhanced their fluorescence effi-

Chart I. Alkyl Benzenepolycarboxylates



ciency. Quite interestingly, benzenehexacarboxylates with bulky alkyl groups showed unexpected dual fluorescence phenomena.

- (1) Preliminary report: Inoue, Y.; Yamasaki, N.; Yokoyama, T.; Tai, A.; Ishida, A.; Takamuku, S. *J. Chem. Soc., Chem. Commun.* **1989**, 1270.
- (2) Baba, H.; Nakajima, A.; Aoi, M.; Chihara, K. *J. Chem. Phys.* **1971**, *55*, 2433. Chihara, K.; Baba, H. *Bull. Chem. Soc. Jpn.* **1975**, *48*, 3093. Chihara, K.; Baba, H. *Chem. Phys.* **1977**, *25*, 299.
- (3) Deinum, T.; Werkhoven, C. J.; Langelaar, J.; Rettschnick, R. P. H.; Van Voorst, J. D. W. *Chem. Phys. Lett.* **1974**, *27*, 206, 552. Langelaar, J.; Leeuw, M. W.; Van Voorst, J. D. W.; Rettschnick, R. P. H. *Ibid.* **1979**, *62*, 14.
- (4) Bark, K. M.; Force, R. K. *J. Phys. Chem.* **1989**, *93*, 7985.
- (5) Majer, J. R.; Al-Saigh, Z. Y. *J. Phys. Chem.* **1984**, *88*, 1157.
- (6) Van der Werf, R.; Schutten, E.; Kommandeur, J. *Chem. Phys.* **1975**, *11*, 281.
- (7) Weller, A. *Z. Phys. Chem. Neue Folge* **1958**, *17*, 224.
- (8) Ito, M.; Inoue, K.; Kuzuhara, T.; Kusui, T. *Bull. Chem. Soc. Jpn.* **1979**, *52*, 14.
- (9) Acuna, A. U.; Amat-Guerri, F.; Catalan, J.; Gonzalez-Tablas, F. *J. Phys. Chem.* **1980**, *84*, 629.
- (10) Heimbrook, L. A.; Kenny, J. E.; Kohler, B. E.; Scott, W. G. *J. Chem. Phys.* **1981**, *75*, 5201.
- (11) Wolfbeis, O. S.; Knierzinger, A.; Schipfer, R. *J. Photochem.* **1983**, *21*, 67.

<sup>†</sup>Himeji Institute of Technology.  
<sup>‡</sup>Osaka University.

In this paper, we discuss the scope and detailed mechanism of this unique dual fluorescence behavior, which is shown to originate from steric hindrance between adjacent bulky substituents.

### Experimental Section

**Instrumentation.** Melting points, measured with a YANACO MP-21 apparatus, are uncorrected. Specific rotations of optically active compounds were determined by using a Perkin-Elmer Model 243B polarimeter with a thermostated cell. Mass spectra were taken on a JEOL AX-500 instrument by fast-atom bombardment (FAB) ionization with or without addition of potassium iodide to the sample.  $^1\text{H}$  and  $^{13}\text{C}$  NMR spectra were recorded at 400 MHz on a JEOL GX-400 spectrometer, using chloroform-*d* or acetone-*d*<sub>6</sub> as a solvent. Infrared spectra were obtained on a JASCO IR-810 instrument.

Electronic absorption and emission spectra were recorded on a JASCO Ubest-50 spectrophotometer and on a JASCO FP-770 spectrofluorometer, respectively. The fluorescence spectra were not corrected for the instrument response function of the spectrometer. Low-temperature spectra were taken at 25 to  $-125$  °C in an Oxford cryostat DN-1704 equipped with a temperature controller ITC-4, or at  $-196$  °C in an immersion-well-type transparent quartz Dewar vessel (Eikosha), filled with liquid nitrogen. Fluorescence lifetimes were measured by means of the time-correlated single photon counting method, using a Horiba NAES-1100 instrument equipped with a pulsed  $\text{H}_2$  light source; the radiation from the lamp was made monochromatic (270 nm) by a 10-cm Jobin-Yvon monochromator, and the emission from a sample was filtered with a Toshiba UV-33 or UV-39 filter.

**Materials.** Pentane was shaken repeatedly with concentrated sulfuric acid until the acid layer no longer turned yellow. The hydrocarbon layer was separated, washed with water, neutralized with sodium carbonate powder, and then distilled fractionally. Acetonitrile was fractionally

distilled from diphosphorus pentoxide.

Commercially available methyl benzoate and dimethyl phthalate, isophthalate, and terephthalate (all from Nakarai) were purified by fractional distillation or recrystallization from ethanol. (–)-Menthol and (–)-borneol were purchased from Nakarai. *tert*-Butyl and menthyl benzoates, dimethyl phthalate and terephthalate, and all 1,2,4,5-benzenetetracarboxylates were prepared from the corresponding acid chlorides and alcohols in pyridine, and purified by repeated distillation or recrystallization from ethanol. Typical procedures of the synthesis are described below for tetramethyl benzenetetracarboxylate.

**(–)-Tetramethyl 1,2,4,5-Benzenetetracarboxylate.** To a stirred pyridine solution (20 mL) of benzenetetracarboxyl tetrachloride (3.00 g, 9.15 mmol), prepared from benzenetetracarboxylic anhydride and phosphorus pentachloride, was added portion-wise (–)-menthol (6.29 g, 40.3 mmol) at room temperature; stirring was continued for 12 h under a nitrogen atmosphere. The reaction mixture was then poured into a mixture of 6% aqueous hydrogen chloride (150 mL) at 5 °C (ice bath) and extracted with three portions of ether (200 mL). The combined organic extracts were washed with saturated aqueous sodium bicarbonate and brine, dried over magnesium sulfate, and then evaporated to dryness under a reduced pressure. The crude product obtained was purified by recrystallization from ethanol to yield pure (–)-tetramethyl 1,2,4,5-benzenetetracarboxylate (5.40 g, 73%): mp 123.5–124.5 °C;  $[\alpha]_{\text{D}}^{20}$   $-102.5^\circ$  (*c* 1.1, benzene); MS (FAB) *m/z* 807 ( $\text{M}^+ + 1$ );  $^1\text{H}$  NMR ( $\text{CDCl}_3$ )  $\delta$  0.82 (d, *J* = 6.8 Hz, 12 H), 0.91 (d, *J* = 6.8 Hz, 12 H), 0.95 (d, *J* = 6.8 Hz, 12 H), 0.85–0.99 (m, 4 H), 1.12 (m, 8 H), 1.40–1.62 (m, 8 H), 1.72 (d, *J* = 11.7 Hz, 8 H), 1.93 (m, 4 H), 2.21 (m, 4 H), 4.94 (t-d, *J* = 11.0, 4.4 Hz, 4 H), 7.93 (s, 2 H); IR (KBr) 2950, 2930, 2870, 1730, 1460, 1300, 1250, 1127, 1100, 958  $\text{cm}^{-1}$ . Anal. Calcd for  $\text{C}_{50}\text{H}_{78}\text{O}_8$ : C, 74.40; H, 9.74. Found: C, 74.18; H, 9.82.

**(–)-Tetraboronyl 1,2,4,5-Benzenetetracarboxylate.** The crude product obtained as above was purified by recrystallization from ethanol: yield 74%; mp 239.5–241.0 °C;  $[\alpha]_{\text{D}}^{20}$   $-59.5^\circ$  (*c* 0.9, benzene); MS (FAB) *m/z* 799 ( $\text{M}^+ + 1$ );  $^1\text{H}$  NMR ( $\text{CDCl}_3$ )  $\delta$  0.90 (s, 12 H), 0.91 (s, 12 H), 0.95 (s, 12 H), 1.21 (d-d, *J* = 14.1, 3.7 Hz, 4 H), 1.26–1.55 (m, 8 H), 1.73–1.80 (m, 8 H), 1.93–2.00 (m, 4 H), 2.47 (m, 4 H), 5.13 (m, 4 H), 8.06 (s, 2 H); IR (KBr) 2970, 2890, 1735, 1460, 1395, 1310, 1280, 1260, 1135, 1105, 1020, 980  $\text{cm}^{-1}$ . Anal. Calcd for  $\text{C}_{50}\text{H}_{70}\text{O}_8$ : C, 75.15; H, 8.83. Found: C, 75.40; H, 9.01.

**Hexamethyl benzenhexacarboxylate** (Tokyo Kasei) was purified by repeated recrystallization from methanol.

The highly congested hexaalkyl esters of benzenhexacarboxylic acid were prepared in the reactions of benzenhexacarbonyl hexachloride with the corresponding alkoxides in the presence of a crown ether. Without crown ether, the esters were not produced in satisfactory yields. Typical procedures are described below for the hexamethyl ester.

**(–)-Hexamethyl Benzenhexacarboxylate.** (–)-Menthol (5.53 g) was added to a benzene suspension (20 mL) of potassium hydride (3.5 g of 35 wt % dispersion in mineral oil, 30.6 mmol) which was washed with dry hexane (5 mL) prior to use; the solution was refluxed for 12 h under a nitrogen atmosphere and then cooled. To the stirred solution was added benzenhexacarbonyl hexachloride (2.00 g, 4.42 mmol) and 18-crown-6 (100 mg). After refluxing for another 24 h under a nitrogen atmosphere, the resultant was allowed to cool, diluted with 6% aqueous hydrogen chloride (200 mL), and then extracted with three portions of ether (200 mL). The combined extracts were washed with saturated aqueous sodium bicarbonate and with brine, dried over magnesium sulfate, and then evaporated under reduced pressure. The crude product obtained was purified by column chromatography over silica gel with hexane–ethyl acetate (97:3) eluent to yield (–)-hexamethyl benzenhexacarboxylate (2.70 g, 53%): mp 128.0–129.5 °C;  $[\alpha]_{\text{D}}^{20}$   $-214.3^\circ$  (*c* 0.31, benzene); MS (FAB (KI)) *m/z* 1209 ( $\text{M}^+ + 39$ );  $^1\text{H}$  NMR ( $\text{CDCl}_3$ )  $\delta$  0.80–1.01 (m, 6 H), 0.81 (d, *J* = 6.8 Hz, 18 H), 0.86 (d, *J* = 6.8 Hz, 18 H), 0.97 (d, *J* = 6.5 Hz, 18 H), 1.10 (m, 12 H), 1.39–1.55 (m, 12 H), 1.70 (m, 12 H), 2.03 (m, 6 H), 2.42 (d, *J* = 12.2 Hz, 6 H), 4.68 (t-d, *J* = 10.7, 4.3 Hz, 6 H);  $^{13}\text{C}$  NMR ( $\text{CDCl}_3$ )  $\delta$  17.21, 21.33, 22.29, 23.70, 25.62, 31.63, 34.32, 39.90, 46.56, 78.84, 134.00, 164.92; IR (KBr) 2950, 2930, 2870, 1740, 1456, 1420, 1240, 1210, 1180, 985  $\text{cm}^{-1}$ . Anal. Calcd for  $\text{C}_{72}\text{H}_{114}\text{O}_{12}$ : C, 73.81; H, 9.81. Found: C, 73.69; H, 9.89. For the fluorescence experiments the product was further purified by recrystallization from ethanol: mp 128.0–129.5 °C.

**Hexaisopropyl benzenhexacarboxylate:** mp 122–123 °C; MS (FAB (KI)) *m/z* 633 ( $\text{M}^+ + 39$ );  $^1\text{H}$  NMR ( $\text{CDCl}_3$ )  $\delta$  1.34 (d, *J* = 6.2 Hz, 36 H), 5.16 (septet, *J* = 6.2 Hz, 6 H);  $^{13}\text{C}$  NMR ( $\text{CDCl}_3$ )  $\delta$  21.59, 70.89, 133.67, 164.61; IR (KBr) 2980, 2940, 2880, 1735, 1425, 1377, 1315, 1255, 1140, 1110, 938, 888, 837  $\text{cm}^{-1}$ . Anal. Calcd for  $\text{C}_{30}\text{H}_{42}\text{O}_{12}$ : C, 60.59; H, 7.12. Found: C, 60.39; H, 7.13.

**Hexa-*tert*-butyl benzenhexacarboxylate:** dp 174–178 °C; MS (FAB (KI)) *m/z* 717 ( $\text{M}^+ + 39$ );  $^1\text{H}$  NMR ( $\text{CDCl}_3$ )  $\delta$  1.57 (s, 54 H);  $^{13}\text{C}$  NMR ( $\text{CDCl}_3$ )  $\delta$  28.35, 84.33, 133.40, 164.93; IR (KBr) 2980, 2930,

- (12) Ikeda, N.; Miyasaka, H.; Okada, T.; Mataga, N. *J. Am. Chem. Soc.* **1983**, *105*, 5206.  
 (13) Van Benthem, M. H.; Gillispie, G. D. *J. Phys. Chem.* **1984**, *88*, 1157.  
 (14) Waluk, J.; Grabowska, A.; Pakula, B.; Sepiol, J. *J. Phys. Chem.* **1984**, *88*, 2954.  
 (15) Ernsting, N. P. *J. Phys. Chem.* **1985**, *89*, 4932.  
 (16) Waluk, J.; Komorowski, S. J.; Herbich, J. *J. Phys. Chem.* **1986**, *90*, 3868.  
 (17) Lakowicz, J. R. *Principles of Fluorescence Spectroscopy*; Plenum: New York, 1983; Chapter 12.  
 (18) Gordon, M.; Ware, W. R., Eds., *The Exciplex*; Academic: New York, 1975.  
 (19) Birks, J. B. *Photophysics of Aromatic Molecules*; Wiley-Interscience: London, 1970; Chapters 7 and 9.  
 (20) Masuhara, H.; Maeda, Y.; Nakajo, H.; Mataga, N.; Tomita, K.; Tatemitsu, H.; Sakata, Y.; Misumi, S. *J. Am. Chem. Soc.* **1981**, *103*, 634.  
 (21) Migita, M.; Okada, T.; Mataga, N.; Sakata, Y.; Misumi, S.; Nakashima, N.; Yoshihara, K. *Bull. Chem. Soc. Jpn.* **1981**, *54*, 3304.  
 (22) Wismontski-Knittel, T.; Das, P. K.; Fischer, E. *J. Phys. Chem.* **1984**, *88*, 1163.  
 (23) Birks, J. B.; Easterly, C. E.; Christophorou, L. G. *J. Chem. Phys.* **1977**, *66*, 4231.  
 (24) Ishikawa, M.; Sugisawa, H.; Fuchikami, T.; Kumada, Y.; Shizuka, H. *J. Am. Chem. Soc.* **1982**, *104*, 2872.  
 (25) Shizuka, H.; Okazaki, K.; Tanaka, H.; Tanaka, M.; Ishikawa, M.; Sumitani, M.; Yoshihara, K. *J. Phys. Chem.* **1987**, *91*, 2057.  
 (26) Nakashima, N.; Inoue, H.; Mataga, N.; Yamanaka, C. *Bull. Chem. Soc. Jpn.* **1973**, *46*, 2288.  
 (27) Struve, W. S.; Rentzepis, P. M. *J. Chem. Phys.* **1974**, *60*, 1533.  
 (28) Wang, Y.; McAuliffe, M.; Novak, F.; Eisenthal, K. B. *J. Phys. Chem.* **1981**, *85*, 3736.  
 (29) Rettig, W. *J. Phys. Chem.* **1982**, *86*, 1970.  
 (30) Rettig, W.; Chandross, E. A. *J. Am. Chem. Soc.* **1985**, *107*, 5617.  
 (31) Okada, T.; Mataga, N.; Baumann, W. *J. Phys. Chem.* **1987**, *91*, 760.  
 (32) Law, K. Y.; Loutfy, R. O. *Macromolecules* **1981**, *14*, 587.  
 (33) Itoh, T.; Kohler, B. E. *J. Phys. Chem.* **1987**, *91*, 1760.  
 (34) Gilabert, E.; Lapouyade, R.; Rulliere, C. *Chem. Phys. Lett.* **1988**, *145*, 262.  
 (35) Lin, C. T.; Guan, H. W.; McCoy, R. K.; Spangler, C. W. *J. Phys. Chem.* **1989**, *93*, 39.  
 (36) Becker, R. S. *Theory and Interpretation of Fluorescence and Phosphorescence*; Wiley: New York, 1969; Chapter 11.  
 (37) Barttrop, J. A.; Coyle, J. D. *J. Chem. Soc. B* **1971**, 251.  
 (38) Baba, H.; Kitamura, M. *J. Mol. Spectrosc.* **1972**, *41*, 302.  
 (39) Acuna, A. U.; Ceballos, A.; Molera, M. J. *J. Chem. Soc., Faraday Trans. 2* **1975**, *72*, 1469.  
 (40) Ghoshal, S. K.; Sarkar, S. K.; Misra, T. N.; Kastha, G. S. *Chem. Phys. Lett.* **1979**, *62*, 503.  
 (41) Baum, J. C. *J. Am. Chem. Soc.* **1980**, *102*, 716.  
 (42) Beriman, I. B. *Handbook of Fluorescence Spectra of Aromatic Molecules*; Academic: New York, 1971; p 58.  
 (43) Inoue, Y.; Yokoyama, T.; Yamasaki, N.; Tai, A. *J. Am. Chem. Soc.* **1989**, *111*, 6480 and the unpublished results.

Table I. Absorption and Fluorescence Spectra of Some Aromatic Carboxylic Esters<sup>a</sup>

aromatic ester	solvent	absorption max/nm	fluorescence	
			maximum/nm	Stokes shift/nm
benzoate				
methyl	pentane	266, 273, 280	<i>b</i>	
<i>tert</i> -butyl	pentane	266, 272, 279	<i>b</i>	
(-)-menthyl	pentane	266, 272, 280	<i>b</i>	
phthalate				
dimethyl	pentane	275, 282	<i>b</i>	
(-)-dimenthyl	pentane	275, 282	<i>b</i>	
isophthalate				
dimethyl	pentane	280, 288	<i>b</i>	
(-)-dimenthyl	pentane	280, 288	<i>b</i>	
terephthalate				
dimethyl	pentane	285, 295	<i>b</i>	
(-)-dimenthyl	pentane	284, 294	<i>b</i>	
1,3,5-benzenetricarboxylate				
trimethyl	pentane	282, 288, (293)	<i>b</i>	
	CH <sub>3</sub> CN	282 (292)	<i>b</i>	
1,2,4,5-benzenetetracarboxylate				
tetramethyl	pentane	283, 291	331	40
	CH <sub>3</sub> CN	291	331	40
(-)-tetrabornyl	pentane	293	331	38
	CH <sub>3</sub> CN	291	331	40
(-)-tetramenthyl	pentane	292	332	40
	CH <sub>3</sub> CN	286, 291	331	40
benzenehexacarboxylate				
hexamethyl	pentane	285, 295	365	70
	CH <sub>3</sub> CN	284, 294	365	71
hexaisopropyl	pentane	283, 293	367	74
hexa- <i>tert</i> -butyl	pentane	286, 295	325, 380	30, 85
			(0.56:1) <sup>c</sup>	
	CH <sub>3</sub> CN	285, 293	325, 385	30, 92
			(0.73:1) <sup>c</sup>	
(-)-hexabornyl	pentane	281, 292	320, 390	28, 98
			(0.03:1) <sup>c</sup>	
	CH <sub>3</sub> CN	280, 290	<i>d</i> , 385	<i>d</i> , 95
(-)-hexamenthyl	pentane	286, 296	335, 365	39, 69
			(0.95:1) <sup>c</sup>	
	CH <sub>3</sub> CN	282, (284), 295	325, 370	30, 75
			(1:1) <sup>c</sup>	
hexadamantyl <sup>e</sup>	ether	295	325, 375	30, 80
			(0.71:1) <sup>c</sup>	

<sup>a</sup> Measured in an aerated solution at room temperature. <sup>b</sup> Fluorescence not detected under the conditions employed. <sup>c</sup> Relative intensity between two maxima. <sup>d</sup> Owing to very poor solubility in acetonitrile, only the major fluorescence peak was unambiguously identified. <sup>e</sup> Practically insoluble in pentane or acetonitrile.

1735, 1477, 1415, 1396, 1370, 1256, 1243, 1150, 1115, 982, 840, 737 cm<sup>-1</sup>. Anal. Calcd for C<sub>36</sub>H<sub>34</sub>O<sub>12</sub>: C, 63.70; H, 8.02. Found: C, 63.71; H, 8.06.

(-)-Hexabornyl benzenehexacarboxylate: mp >300 °C; [α]<sub>D</sub><sup>20</sup> -2.81° (c 0.31, benzene); MS (FAB (KI)) *m/z* 1197 (M<sup>+</sup> + 39); <sup>1</sup>H NMR (CDCl<sub>3</sub>) δ 0.87 (s, 18 H), 0.90 (s, 18 H), 0.93 (s, 18 H), 1.23–1.35 (m, 18 H), 1.65–1.77 (m, 12 H), 1.96 (m, 6 H), 2.37 (m, 6 H), 5.20 (d, *J* = 9.3 Hz, 6 H); <sup>13</sup>C NMR (CDCl<sub>3</sub>) δ 14.14, 18.92, 19.81, 27.24, 27.83, 35.87, 44.85, 48.15, 49.38, 83.85, 133.44, 165.55; IR (KBr) 2960, 2880, 1740, 1456, 1420, 1247, 1215, 1115, 1014 cm<sup>-1</sup>. Anal. Calcd for C<sub>72</sub>H<sub>102</sub>O<sub>12</sub>: C, 74.58; H, 8.87. Found: C, 73.78; H, 8.89.

Hexa-1-adamantyl benzenehexacarboxylate: mp >300 °C; MS (FAB (KI)) *m/z* 1185 (M<sup>+</sup> + 39); <sup>1</sup>H NMR (CDCl<sub>3</sub>) δ 1.67 (m, 36 H), 2.20 (br s, 18 H), 2.27 (br s, 36 H); <sup>13</sup>C NMR (CDCl<sub>3</sub>) δ 31.15, 36.34, 41.49, 84.51, 133.23, 164.58; IR (KBr) 2910, 2850, 1735, 1458, 1415, 1355, 1220, 1050, 963, 864 cm<sup>-1</sup>. Anal. Calcd for C<sub>72</sub>H<sub>90</sub>O<sub>12</sub>: C, 75.36; H, 7.91. Found: C, 74.98; H, 7.90.

## Results and Discussion

**Absorption Spectra.** In Table I are listed the absorption maxima around 280 nm of benzenemono-, 1,2-, 1,3-, and 1,4-benzenedi-, 1,3,5-benzenetri-, 1,2,4,5-benzenetetra-, and benzenehexacarboxylates of methyl and some bulky alcohols. Although each absorption band becomes broader in the highly substituted esters, the 0–0 band can be assigned as the longest wavelength peak in the spectrum.

As shown in Table I, the apparent 0–0 band shifts in general to longer wavelengths as the number of alkoxy carbonyl substituent(s) introduced increases. However, the bathochromic shift

induced is a critical function of the degree of π-conjugation between the benzene and carbonyl chromophores. Thus the phthalates show much smaller bathochromic shifts (2 nm) than those for the iso- and terephthalates (8 and 15 nm, respectively). This may be attributed to the steric hindrance between the ortho carbonyl groups, leading to partial deconjugation of the π system. A similar but much evident deconjugating effect by ortho substitution is seen in the spectra of tetra- and hexacarboxylates; the absorption 0–0 bands of these sterically congested polycarboxylates are very close in energy to those of the less substituted, but strain-free, terephthalates and 1,3,5-benzenetricarboxylate.

**Fluorescence Spectra.** The fluorescence behavior of various mono- to hexacarboxylates is summarized in Table I. No appreciable emission from mono-, di-, and tricarboxylates was detected in fluid solutions at room temperature under our experimental conditions; i.e., aerated or argon-saturated samples at 10<sup>-4</sup>–10<sup>-6</sup> M concentrations and a conventional fluorometer at the highest sensitivity with the widest excitation and emission slit openings of 10 nm. However, 1,2,4,5-benzenetetracarboxylates were found to emit weak fluorescence around 331 nm; their fluorescence excitation spectra were in excellent agreement with the absorption spectra. Naturally, all tetracarboxylates with a variety of alcohol moieties afforded almost identical absorption 0–0 band maxima (ca. 292 nm) and fluorescence maxima (331 nm), irrespective of the bulkiness of alcohol moieties.

Interestingly, the fluorescence behavior of hexacarboxylates was completely different, depending evidently on the bulkiness

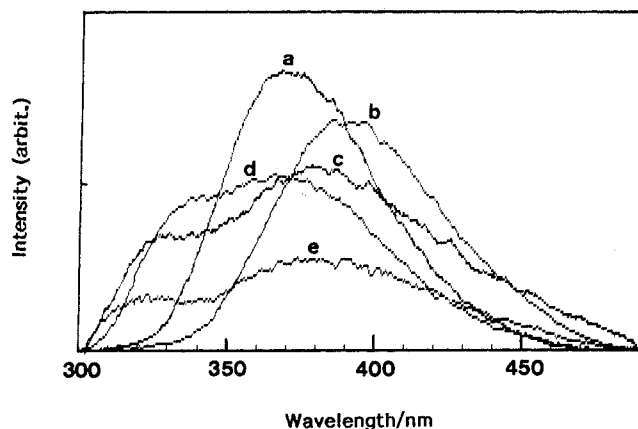


**Figure 1.** Fluorescence spectra of (a) hexamethyl ( $1.0 \times 10^{-5}$  M in aerated pentane), (b) (–)-hexabornyl ( $2.1 \times 10^{-5}$  M in aerated pentane), (c) hexadamantyl benzenhexacarboxylate ( $2.0 \times 10^{-5}$  M in aerated ether), (d) (–)-hexamenthyl ( $1.8 \times 10^{-5}$  M in aerated pentane), and (e) hexa-*tert*-butyl benzenhexacarboxylate ( $2.1 \times 10^{-5}$  M in aerated pentane): temp 25 °C, excitation wavelength 250 nm.

of alkyl groups. The less bulky methyl ester exhibited single fluorescence peak at 365 nm with a large Stokes shift of 70 nm, indicating that substantial conformational relaxation takes place in the excited state. By contrast, highly congested *tert*-butyl, bornyl, menthyl, and adamantyl esters gave distinct two peaks at different wavelengths with small and very large Stokes shifts, which are obviously related to the alkyl group introduced; see Figure 1 and Table I. It is interesting to note that, possessing a close partial structure, *tert*-butyl and 1-adamantyl esters, traces e and c, show very similar fluorescence spectra. The isopropyl ester is an intermediate case; although no appreciable dual fluorescence was detected at room temperature, a very weak but unambiguous new emission peak emerged out around 325 nm at low temperatures, in addition to the existing long-wavelength peak at 367 nm, as described later. Importantly, the excitation spectra taken at both fluorescence maxima were absolutely identical with each other and also to the absorption spectrum in all but isopropyl and bornyl cases, for which the short-wavelength peak was too weak to measure its excitation spectrum, at least at the room temperature. Thus the possible intervention of any ground-state conformer or monomer/complex pair as the origin of dual fluorescence is ruled out, on condition that these pairs possess different absorption spectra. Furthermore, there was no concentration effect; the shape and relative intensity of dual fluorescence peaks from menthyl hexacarboxylate were independent of the sample concentration over a range of  $10^{-4}$  to  $10^{-6}$  M.

Since the absorption 0–0 band maxima do not differ substantially among these hexacarboxylates, the observation of dual fluorescence peaks indicates that, in these sterically congested esters, at least two excited states of different energies are involved, and also that the conversion from one to another is decelerated to such a rate that is comparable with those of the radiative and nonradiative deactivation processes. Taking into account the facts that only the sterically congested esters showed dual peaks and that virtually no concentration effect was observed, the different emitting states involved are not an excited monomer/excimer fluorophore pair but are most likely the conformational isomers of the excited singlet, rotational relaxation of which is restricted by the steric hindrance between the adjacent bulky alcohol moieties of hexacarboxylates.

From the observed absorption 0–0 bands very close in energy to those of terephthalates, the hexacarboxylates are inferred to possess staggered, less conjugating structure with respect to alkoxy-carbonyl groups owing to steric hindrance. In fact, X-ray crystallographic studies<sup>44,45</sup> revealed that the crystal of hexamethyl

benzenhexacarboxylate consists of two crystallographically independent molecules, and the torsion angles of six methoxy-carbonyl groups to the benzene ring are not uniform in each molecule, varying from 53 to 65° or from 46 to 66°,<sup>45</sup> respectively. On the other hand, possible structural changes upon excitation were evaluated through semiempirical MO calculations on methyl benzoate, using the MNDOC program,<sup>46</sup> since the attempted calculations on the tetra- and hexacarboxylates, starting with several different initial structures, could not achieve self-consistence on the program, probably owing to the inappropriate initial structures and the severe steric and/or inappropiate interaction between the ortho substituents. However, MNDOC calculations on methyl benzoate in the ground and excited singlet states revealed that the bond lengths of the aromatic C1–C2 and C3–C4 bonds decrease slightly (0.01 Å) in the excited state, while the aromatic C2–C3 bond, in particular, and the C1–C(=O) bond are contrarily elongated by 0.07 and 0.01 Å, respectively; no significant changes were observed in the other bonds or angles. These sorts of bond elongations and structural changes, which are expected to occur also in the other benzenepolycarboxylates upon excitation, may facilitate rotational relaxation about some single bonds, which has been restricted in the ground electronic state. Thus, the short- and long-wavelength fluorescence peaks are reasonably assigned to the emissions from the near-Franck-Condon (FC') and fully relaxed (RX) singlet states, respectively. The relative intensity of the two peaks, shown in the parentheses in Table I, is a certain measure of both the relative population of the FC' and RX singlets and the feasibility of rotational relaxation in the excited state.

**Solvent Effect.** In two typical nonpolar and polar aprotic solvents, the absorption spectra were measured with tri-, tetra-, and hexacarboxylates. As can be seen from Table I, essentially no significant spectral changes were observed in the absorption spectra in the solvents of different polarity, indicating trivial contribution of polar structure and negligible solute–solvent dipolar interaction for these benzenepolycarboxylates, at least in the ground electronic state.

The fluorescence spectra were also fairly insensitive to solvent polarity. For all tetracarboxylates and methyl hexacarboxylate, which show usual single fluorescence peaks with moderate to large Stokes shifts, virtually no significant changes in fluorescence spectrum were observed in the typical nonpolar and polar aprotic solvents; see Table I. Similarly, the position and relative intensity of dual fluorescence maxima of the highly congested hexacarboxylates changed only slightly with solvent polarity. It is thus deduced from the present results that the emitting state(s) of benzenepolycarboxylates, whether single or dual, are inherently nonpolarized and are mostly  $\pi, \pi^*$  in nature. Since the dual fluorescence arising from the twisted intramolecular charge-transfer (TICT) mechanism are known to be sensitive to the solvent polarity,<sup>26–35</sup> the negligible solvent effect observed clearly eliminates possible involvement of the TICT mechanism to rationalize this novel dual fluorescence phenomena.

**Temperature Effect.** The fluorescence spectra of hexacarboxylates were measured in pentane at various temperatures ranging from 25 to –125 °C. Typical temperature-dependent fluorescence spectra are illustrated for some benzenhexacarboxylates in Figure 2.

The fluorescence intensity of methyl ester increases gradually with lowering temperature down to –50 °C, but then decreases drastically below –75 °C, as shown in Figure 2a. This abrupt drop in intensity is simply due to the low solubility of the methyl

(45) An independent X-ray crystallographic study by K. Morioka, M. Yasuda, and K. Shima of Miyazaki University, using our crystals of hexamethyl benzenhexacarboxylate, afforded essentially identical structures with those reported in ref 44, except for somewhat different torsion angles of 48 to 63 and 46 to 64°. A similar study on the hexamenthyl ester is currently under way, but results are unsuccessful so far; the full details of these studies will be published elsewhere.

(46) The MNDOC program, released through QCPE (No. 353), was run on a Fujitsu S-3500 computer to obtain the fully optimized structures in the ground and excited states.

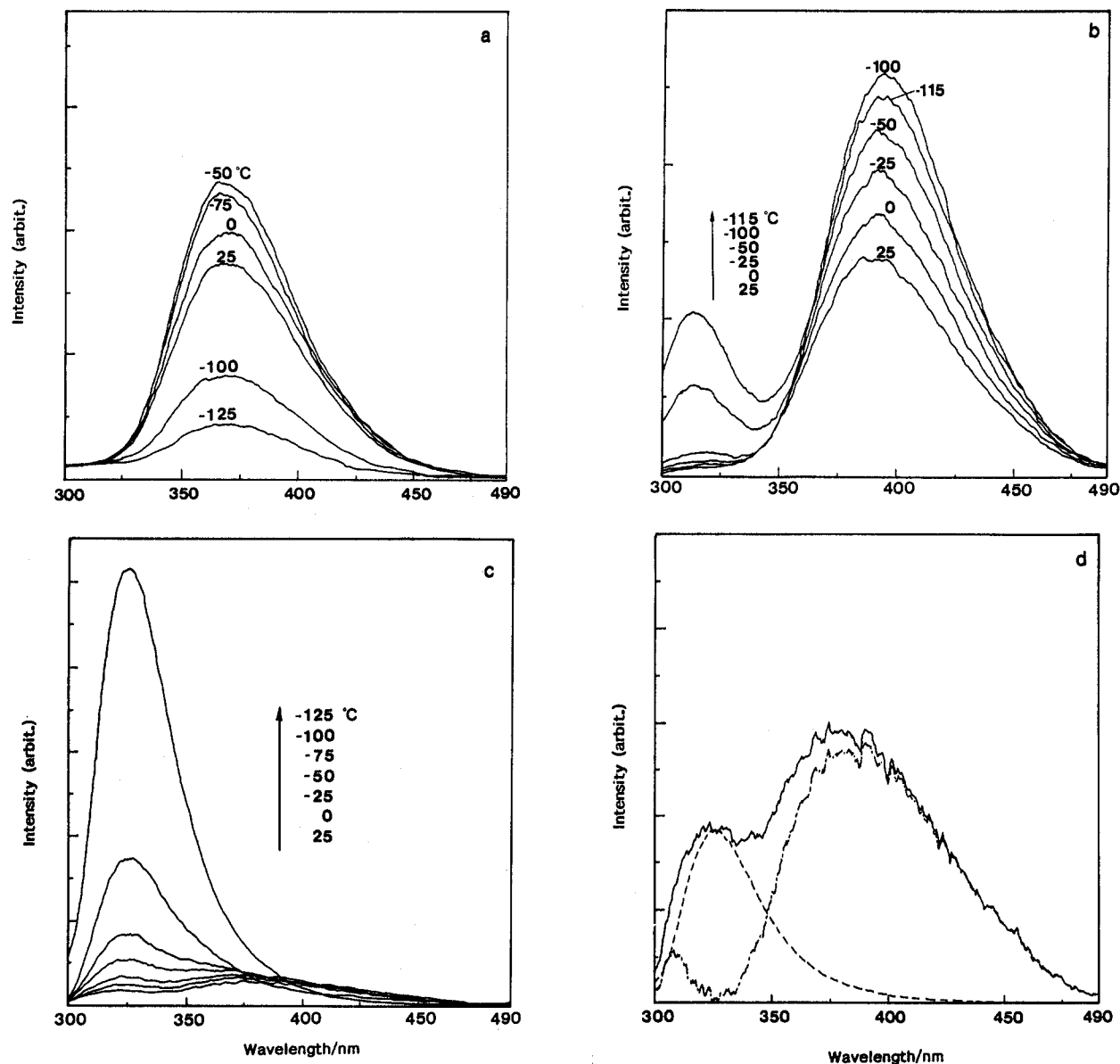


**Figure 2.** Temperature dependence of fluorescence spectra of (a) hexamethyl, (b) (-)-hexabornyl, and (c) hexa-*tert*-butyl benzenehexacarboxylates in argon-saturated pentane at 25 to -115 or -125 °C; (d) deconvolution of dual fluorescence of the *tert*-butyl ester at 25 °C with its single-peak spectrum at -125 °C.

ester, particularly at low temperatures. It is important, however, that the shape and position of the fluorescence peak did not change throughout the temperature range examined and no new peak(s) emerged out with this less congested methyl ester.

In the bornyl case shown in Figure 2b, the short-wavelength peak, which is appreciable but extremely weak at room temperature, grows dramatically to afford a distinct intense peak at 320 nm with concomitant moderate increases in intensity of the long-wavelength peak at 390 nm down to -100 °C. Upon further cooling down to -115 °C, the peak at 320 nm continues to grow at the expense of the 390-nm peak. Not shown in the figure, the temperature dependence of isopropyl ester resembles the bornyl case, although the short-wavelength peak around 325 nm is not evident at room temperature and its development at lower temperatures is much less dramatic.

*tert*-Butyl and menthyl esters, both of which show evident dual fluorescence peaks of comparable intensities at room temperature, behave similarly. As shown in Figure 2c for the *tert*-butyl ester, the rapid growth of short-wavelength peak at low temperatures makes contribution of the long-wavelength peak negligible, affording an apparent single fluorescence peak at temperatures below -100 °C. Deconvolution of the spectrum at each temperature using the single-peak spectrum at -125 °C allows us to separate

two peaks, as exemplified in Figure 2d.

The temperature effects upon the NMR spectrum were also studied, since the fluorescence-spectral changes upon cooling would originate from the equilibrium shift between a hypothetical ground-state conformer or monomer/complex pair that fluoresce independently to afford the dual fluorescence. However, the variable-temperature NMR spectra of *tert*-butyl and menthyl hexacarboxylates in chloroform-*d* or acetone-*d*<sub>6</sub> did not manifest the presence of such a conformer or complex at 20, -60, and -90 °C.

**Dual Fluorescence Model.** From the above experiments, it is shown that this novel dual fluorescence system involves two energetically separated emitting states, i.e., the near-Frank-Condon (FC') and fully relaxed (RX) singlet states. The temperature-dependence study indicates that the relaxation process in fluid solution requires some activation energy depending upon the steric hindrance caused by bulky alkyl groups. Thus, the stepwise relaxation of the initially formed FC state to the FC' and then to the final RX state may be illustrated as shown in Figure 3, where  $k_f$  and  $k_d$  refer to the rate constants for fluorescent and nonradiative decays, respectively, and  $k_r$  for conformational relaxation from FC' to RX state; the intersystem crossing processes ( $k_{isc}$ ) from FC' and RX states to the corresponding triplet excited

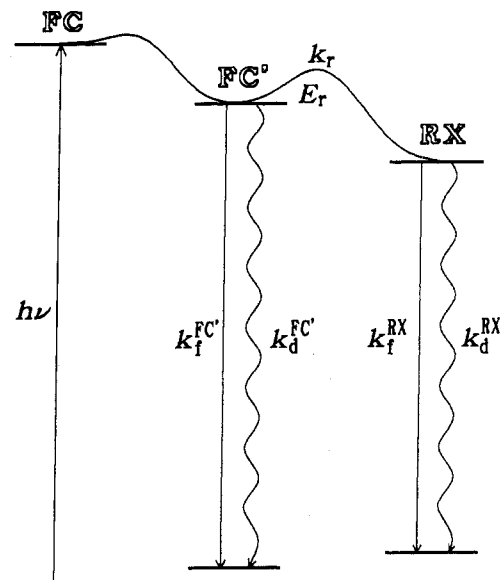


**Figure 3.** Dual fluorescence model: schematic relaxation processes for excited singlet of benzenehexacarboxylates with bulky alkyl groups; FC, FC', and RX refer to Franck-Condon, Franck-Condon-like, and relaxed excited states, respectively.

states are not shown in Figure 3 for simplicity.

According to the above sequence, the fluorescence quantum yields of the short- and long-wavelength peaks are given by the following equations, where the intersystem crossing processes ( $k_{isc}$ ) from the FC' and RX states are also taken into account.

$$\Phi_f^{FC'} = k_f^{FC'} / (k_f^{FC'} + k_d^{FC'} + k_{isc}^{FC'} + k_r)$$

$$\Phi_f^{RX} = [k_r / (k_f^{FC'} + k_d^{FC'} + k_{isc}^{FC'} + k_r)] \times [k_f^{RX} / (k_f^{RX} + k_d^{RX} + k_{isc}^{RX})]$$

Then the relative intensity of the dual fluorescence peaks is expressed as follows:

$$\Phi_f^{FC'} / \Phi_f^{RX} = (k_f^{FC'} / k_r) [(k_f^{RX} + k_d^{RX} + k_{isc}^{RX}) / k_f^{RX}] \quad (1)$$

Since, in the temperature-dependence study, the long-wavelength peak of bulky hexacarboxylates showed only small increase or even decrease in intensity upon cooling, we may assume that the sum of fluorescence and intersystem crossing processes from the RX state is much faster than the nonradiative decay, i.e.,  $k_f^{RX} + k_{isc}^{RX} \gg k_d^{RX}$ . Then the eq 1 is reduced to

$$\Phi_f^{FC'} / \Phi_f^{RX} = (k_f^{FC'} / k_r) [(k_f^{RX} + k_{isc}^{RX}) / k_f^{RX}] \quad (2)$$

Further assuming temperature-independent fluorescence and intersystem-crossing rate constants ( $k_f$  and  $k_{isc}$ ), and applying the Arrhenius equation to the relaxation rate constant  $k_r$ , we obtain:

$$\ln (\Phi_f^{FC'} / \Phi_f^{RX}) = E_r / RT - \ln A_r + \ln k_f^{FC'} (k_f^{RX} + k_{isc}^{RX}) / k_f^{RX} \quad (3)$$

The natural logarithm of the relative fluorescence intensity obtained in the temperature-dependence study was plotted against the reciprocal temperature to give a good straight line for each bulky alkyl hexacarboxylates as shown in Figure 4. From the slope of plot, the energy of activation ( $E_r$ ) for the relaxation from FC' to the RX state can be calculated for each bulky alkyl hexacarboxylate. The activation energies  $E_r$  obtained for the methyl, isopropyl, bornyl, *tert*-butyl, and menthyl esters are  $\sim 0$ , 0.3, 1.8, 2.1, and 2.5 kcal/mol, respectively. These values may be taken as a quantitative measure of steric hindrance and viscous drag caused by the solvent for rotational relaxation of the bulky alkyl hexacarboxylates in the excited state.

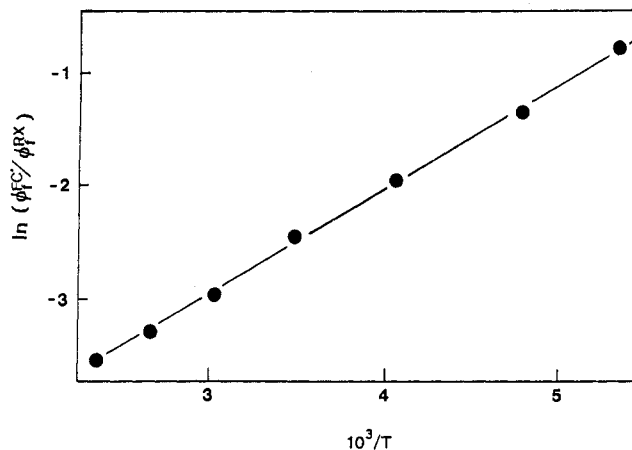


**Figure 4.** Logarithm of relative intensity of short- and long-wavelength peaks as a function of reciprocal temperature for hexabornyl benzenehexacarboxylate.

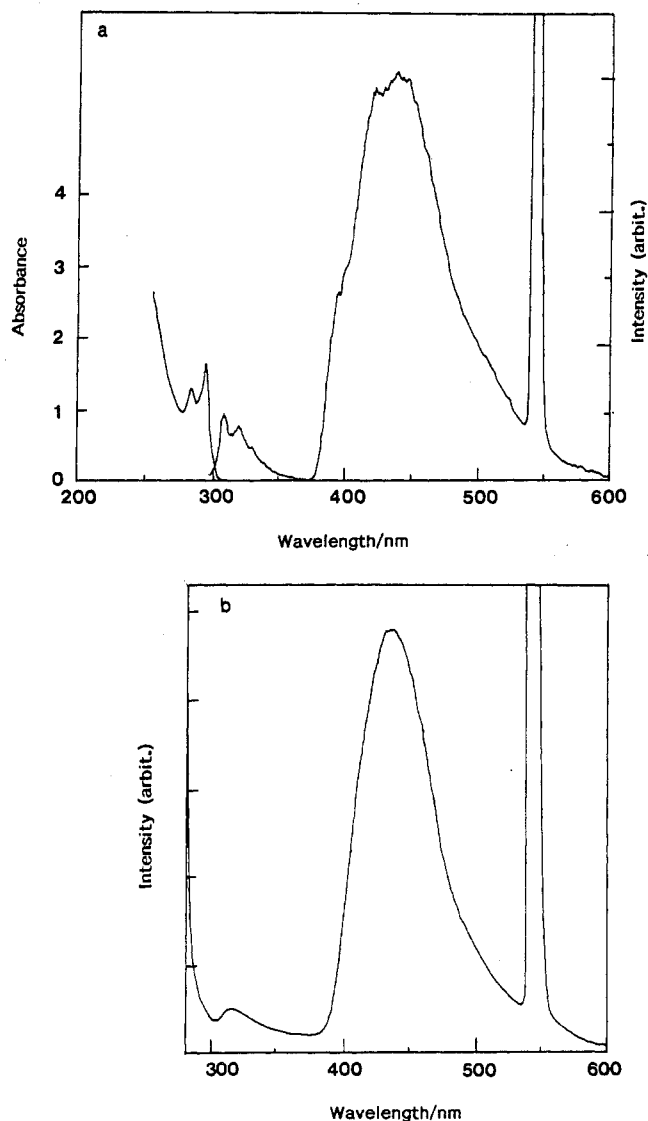


**Figure 5.** (a) Absorption (left trace;  $5.4 \times 10^{-4}$  M) and emission (right trace;  $2.1 \times 10^{-5}$  M) spectra of hexa-*tert*-butyl benzenehexacarboxylate in nitrogen-saturated isopentane-methylcyclohexane (3:1) matrix at  $-196$  °C; (b) solid-state reflective emission spectrum of hexa-*tert*-butyl benzenehexacarboxylate powder at room temperature under aerial condition; the large spike around 540 nm is the second harmonic of exciting radiation.

**Matrix Isolation.** Absorption and emission spectra of some tetra- and hexacarboxylates were measured in glass matrices at

**Table II.** Absorption, Fluorescence, and Phosphorescence Spectra of Some Aromatic Esters in Rigid Matrix at  $-196\text{ }^{\circ}\text{C}^a$ 

aromatic ester <sup>b</sup>	matrix	absorption max/nm <sup>c</sup>	fluorescence max/nm <sup>c</sup>	phosphorescence max/nm <sup>c</sup>	rel intensity <sup>d</sup>
1,2,4,5-benzenetetracarboxylate					
methyl	IP-MCH	285, 294	323 <sup>e</sup>	453 <sup>e</sup>	4.9
bornyl	IP-MCH	287, 295	309, 318	438 <sup>e</sup>	3.8
menthyl	IP-MCH	290, 297	312, 323	448 <sup>e</sup>	1.0
benzenehexacarboxylate					
methyl	IP-MCH	281, 295	322, 335 (348)	(400) 423 (448)	6
	MTHF	281, 293	302, 312 (324)	388, 410, 434	9.7
isopropyl	MTHF	280, 292	300, 312 (323)	390, 415, 433	18.5
<i>tert</i> -butyl	IP-MCH	285, 296	307, 318 (329)	(395) 418, 438	31.3
bornyl	IP-MCH	280 (290)	302, 312, 321	384, 406, 428	6.3
menthyl	IP-MCH	284, 294	300, 311 (322)	394, 415, 437	7.8

<sup>a</sup> Measured in aerated 3:1 isopentane-methylcyclohexane (IP-MCH) or 2-methyltetrahydrofuran (MTHF) matrix. <sup>b</sup> Sample concentrations employed were mostly around  $10^{-4}$  except for the samples of poor solubility, with which concentrations around  $10^{-6}$  M were used. <sup>c</sup> Shoulder peaks in parentheses. <sup>d</sup> Apparent relative intensity of phosphorescence-fluorescence (uncorrected). <sup>e</sup> Diffused broad peak.

$-196\text{ }^{\circ}\text{C}$ , mostly using a 3:1 isopentane-methylcyclohexane (IP-MCH) mixture or 2-methyltetrahydrofuran (MTHF) as organic glass.

As a typical example, the absorption and emission spectra of *tert*-butyl hexacarboxylate are shown in Figure 5a (the large spike around 540 nm is the second harmonic of exciting radiation). As expected, each absorption band is sharp and well-separated in the rigid matrix, while the absorption maximum shows only small or negligible hypsochromic shifts as compared with those in the fluid solution at room temperature; compare the corresponding data in Tables I and II. In the emission spectrum, well-separated fluorescence peaks and much intense phosphorescence peaks were observed at wavelengths around 300 and 400 nm, respectively. The excitation spectra, measured at the fluorescence and phosphorescence maxima, agreed exactly with the absorption spectrum. The other hexacarboxylates also afforded analogous emission spectra, as summarized in Table II. The detailed shape and position of individual peaks, as well as the relative intensity between fluorescence and phosphorescence, varied with the alkyl groups introduced. On the other hand, the tetracarboxylates gave diffuse fluorescence and phosphorescence peaks (Table II).

In contrast to their usual fluorescence behavior in fluid solutions, all the hexacarboxylates in glass matrices behave in a "normal" manner, giving mirror images between the absorption and fluorescence spectra, and never show any sign of dual fluorescence. This is attributed solely to the restricted molecular motions in glass matrices. The solid-state reflective emission spectrum of a powder sample of *tert*-butyl hexacarboxylate was also measured at room temperature to give quite similar, but structureless, spectrum, as shown in Figure 5b.

It is interesting to note that the emission spectra of methyl hexacarboxylate depends on the matrix rigidity to some extent. Thus, small hypsochromic shifts of fluorescence and phosphorescence 0-0 bands were observed even at  $-196\text{ }^{\circ}\text{C}$  by changing the matrix from less rigid IP-MCH to highly rigid MTHF; see the data for methyl benzenehexacarboxylate in Table II. The fluorescence 0-0 band of the methyl ester in the rigid MTHF matrix is very close to those of other highly bulky hexacarboxylates in IP-MCH matrices. Hence it is deduced that at least methyl, and probably isopropyl, ester molecules in the excited state are allowed to move to some extent in a soft glass matrix like IP-MCH even at  $-196\text{ }^{\circ}\text{C}$ , but no longer in a rigid matrix like MTHF.

Successive emission measurements of the matrix-isolated hexacarboxylate during its thawing process gave useful insights into this relaxation process and may connect the observations in matrices and in fluid solutions at low temperatures. An IP-MCH (4:1) matrix containing *tert*-butyl hexacarboxylate was prepared in a Dewar vessel as usual, and then the coolant liquid nitrogen in the vessel was discarded to initiate gradual thawing within several minutes. Subsequent changes in the emission spectrum were recorded repeatedly at ca. 1-min intervals. The resulting spectral changes are shown in Figure 6 (the large spike around 540 nm is the second harmonic of exciting radiation). Once thawing starts, the emission spectrum changes dramatically within

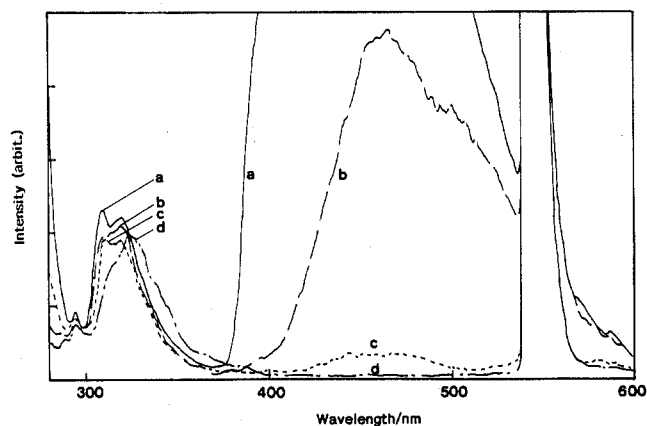


**Figure 6.** Spectral changes during natural thawing of isopentane-methylcyclohexane (4:1) matrix containing hexa-*tert*-butyl benzenehexacarboxylate ( $2.0 \times 10^{-5}$  M) upon warming from  $-196\text{ }^{\circ}\text{C}$ . A series of spectra a-d were taken successively at ca. 1-min interval just after the change began (trace a); the large spike around 540 nm is the second harmonic of exciting radiation.

the first 3-4 min. At time zero (Figure 6, trace a), the spectrum retains the original shapes and intensities in both fluorescence and phosphorescence regions. Within a few minutes (traces b-d), the fluorescence peak shifts to longer wavelengths with a loss of structure, while the phosphorescence peak completely fades out, indicating thorough liquefaction of the glass matrix. The fluorescence maximum at 325 nm obtained after ca. 3 min of thawing (trace d) coincides with the short-wavelength peak of dual fluorescence at room temperature, but no long-wavelength peak is seen at this temperature just above the melting point of the IP-MCH (4:1) mixture around  $-160\text{ }^{\circ}\text{C}$ , as is the case with the fluorescence spectrum taken at  $-125\text{ }^{\circ}\text{C}$  in pentane. Thus, the thawing experimental enables us to observe separately the first relaxation process from the FC to FC' state and also to assign unambiguously the short-wavelength peak of dual fluorescence not to the literal Franck-Condon (FC) state but to the partially relaxed near-Franck-Condon (FC') state.

**Lifetime Measurement.** Fluorescence lifetimes ( $\tau$ ) of some tetra- and hexacarboxylates were measured in fluid solutions at room and low temperatures by the time-correlated single-photon counting method. Owing to the substantially low emission efficiencies of these polycarboxylates, full emission from the sample was detected in most measurements through a UV-33 filter (0% transmittance ( $T$ ) at  $<300$  nm; 50%  $T$  at 330 nm), while some experiments were conducted with a UV-39 filter (0%  $T$  at  $<360$  nm; 50%  $T$  at 390 nm) in order to measure the lifetime of long-wave-length fluorescence separately.

As can be seen from Table III, the tetracarboxylates gave fairly short lifetimes around 0.2 ns, which were not affected by the solvent polarity. On the other hand, the hexacarboxylates gave somewhat longer lifetimes of 0.5-1.1 ns, and the solvent polarity

**Table III.** Fluorescence Lifetimes of Some Tetra- and Hexacarboxylates in Fluid Solution

aromatic ester	solvent	atm	temp, °C	filter	lifetime <sup>a</sup> /ns
1,2,4,5-benzenetetracarboxylate					
tetramethyl	pentane	air	22	UV-33	0.2
	CH <sub>3</sub> CN	air	21	UV-33	0.2
(-)-tetraboranyl	pentane	air	24	UV-33	0.2
(-)-tetramenthyl	pentane	air	23	UV-33	0.3
benzenehexacarboxylate					
hexamethyl	pentane	air	25	UV-33	1.1
		argon	25	UV-33	1.1
	CH <sub>3</sub> CN	air	23	UV-39	0.6
hexaisopropyl	pentane	air	25	UV-33	1.0
hexa- <i>tert</i> -butyl	pentane	air	23	UV-33	0.5
		air	23	UV-39	0.5
(-)-hexaboranyl	pentane	air	28	UV-33	1.1
		argon	23	UV-33	1.1
		argon	23	UV-39	1.1
		argon	-125	UV-33	1.6
(-)-hexamenthyl	pentane	air	24	UV-33	0.7
		air	24	UV-39	0.7

<sup>a</sup> Experimental error  $\pm 0.1$ – $0.2$  ns.

affected to a small extent in the methyl ester case. The short lifetimes make the fluorescence behavior of these polycarboxylates insensitive to the atmosphere;<sup>42</sup> indeed, both air- and argon-saturated sample solutions showed no appreciable changes in fluorescence lifetime or in shape and intensity of the fluorescence spectrum.

Unexpectedly, the decay profile of dual fluorescence from *tert*-butyl and menthyl hexacarboxylates, measured through a UV-33 filter, was analyzed successfully by the convolution procedures assuming a one-component, single-exponential curve, rather than two-component, double-exponential curves, in all cases. Furthermore, the use of a UV-39 filter, which does not transmit any radiation below 360 nm and permits sole detection of the long-wavelength fluorescence of these hexacarboxylates, gave the same lifetimes as those obtained above within experimental error (Table III). It is thus inferred that the two emitting states possess quite similar lifetimes or equilibrate very rapidly, or the short-wavelength fluorescence possesses extremely short lifetime beyond the time resolution of the instrument ( $\sim 0.2$  ns).

The fluorescence lifetime of bornyl hexacarboxylate was measured at  $-125$  °C with excitation at 270 nm. Although the ester showed evident dual fluorescence at low temperatures (Figure 2b), the decay profile was single-exponential and the lifetime was elongated only slightly to 1.6 ns, indicating a small contribution of nonradiative thermal deactivation from the fluorescing state.

**Quenching Experiment.** Fluorescence-quenching experiments afforded further valuable insights into the dual-fluorescing FC' and RX states. The fluorescence from polycarboxylates was quenched fairly efficiently by simple alkenes like cyclooctene. As exemplified in Figure 7a for the quenching of dual fluorescence from menthyl hexacarboxylate with (*Z*)-cyclooctene, the long-wavelength peak was quenched more efficiently than the short-wavelength one. A conventional Stern–Volmer plot of the relative fluorescence intensity ( $\Phi_f^0/\Phi_f$ ) in the absence and presence of

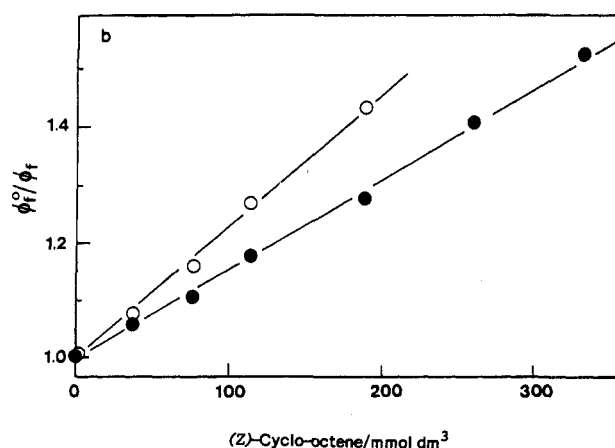
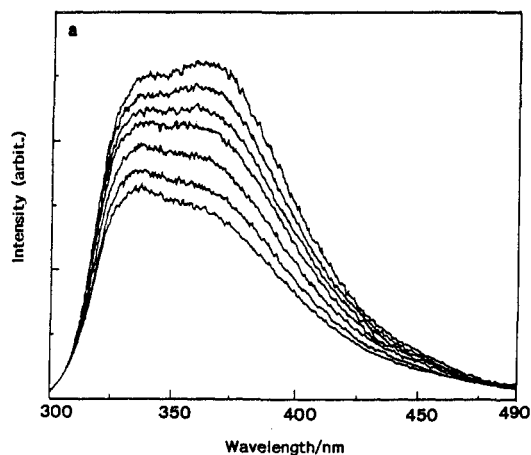


**Figure 7.** (a) Quenching of dual fluorescence from (-)-hexamenthyl benzenehexacarboxylate ( $2.1 \times 10^{-3}$  M) with (*Z*)-cyclooctene (0–0.331 M, from top to bottom) in aerated pentane at 25 °C and (b) Stern–Volmer plot for the quenching of the short- (●) and long-wavelength (○) peaks.

quencher against the quencher concentration gave an excellent straight line for each peak as shown in Figure 7b; the Stern–Volmer constant ( $k_q\tau$ ) is given as a slope. Similar quenching experiments were carried out with *tert*-butyl hexacarboxylate; the results are listed in Table IV.

Significantly, the short- and long-wavelength peaks of dual fluorescence behave independently to give distinctly different Stern–Volmer constants in the quenching with *Z* and *E* isomers of cyclooctene. This clearly rules out the above-mentioned hypothesis assuming a rapid equilibrium between two emitting states, which could rationalize the single-exponential decay observed for dual fluorescence. Thus the lifetimes of two emitting states, i.e., FC' and RX, are inferred to possess comparable lifetimes in all cases examined, at least within the present time resolution ( $\sim 0.2$  ns), although the extremely short-lived excited state is not rigorously excluded.

**Table IV.** Independent Quenching of Dual Fluorescence Peaks from Hexaalkyl Benzenehexacarboxylates by (*E*)- and (*Z*)-Cyclooctene<sup>a</sup>

alkyl	lifetime/ns	obsd wavelength/nm	$k_{qE}\tau^b$	$k_{qZ}\tau^c$	$k_{qE}^d/10^9$	$k_{qZ}^d/10^9$	$k_{qE}/k_{qZ}^e$
<i>tert</i> -butyl	0.5	325	2.17	0.34	4.3	0.7	6.4
		380	4.15	0.90	9.3	1.8	4.6
		$k_q^{380}/k_q^{325f}$	1.91	2.65			
menthyl <sup>g</sup>	0.7	332	3.04	1.59	4.3	2.3	1.9
		372	4.33	2.38	6.2	3.4	1.8
		$k_q^{372}/k_q^{332f}$	1.42	1.50			

<sup>a</sup> Measured with  $2.1 \times 10^{-4}$  M solution of hexacarboxylate in aerated pentane at 25 °C. <sup>b</sup> Stern–Volmer constant in  $M^{-1} s^{-1}$ , obtained by quenching with 0.019–0.188 M (*E*)-cyclooctene. <sup>c</sup> Stern–Volmer constant in  $M^{-1} s^{-1}$ , obtained by quenching with 0.038–0.435 M (*Z*)-cyclooctene. <sup>d</sup> Calculated from Stern–Volmer constant, assuming the same lifetime for the short- and long-wavelength fluorescences. <sup>e</sup> Relative quenching rate constant between *E* and *Z* isomers. <sup>f</sup> Relative quenching rate constant between long- and short-wavelength peaks, or RX and FC' states. <sup>g</sup> Intensity changes of the short- and long-wavelength peaks were measured not at peak tops but at 332 and 372 nm in order to avoid the influence of mutual overlap.

Using the lifetimes obtained above, the individual quenching rate constants  $k_q$  for the *E* and *Z* isomers of cyclooctene are calculated for the hexacarboxylates. As shown in Table IV, the quenching rate constants for (*E*)-cyclooctene, being fairly close to the diffusion rate constant, are 1.8–6.5 times greater than those for the *Z* isomer, probably owing to the much lower ionization potential<sup>47,48</sup> or singlet energy<sup>49</sup> of the *E* isomer. Significantly,

(47) Batch, C.; Ermer, O.; Heilbronner, E.; Wiseman, J. R. *Angew. Chem.* 1973, 85, 302.

(48) Robin, M. B.; Taylor, G. N.; Kuebler, N. A. *J. Org. Chem.* 1973, 38, 1049.

the quenching rate constants for both *E* and *Z* isomers differ not only with the bulkiness of alkyl group but also with the excited state to be quenched, i.e., FC' and RX, indicating that these two states bear considerable structural differences.

**Acknowledgment.** This work was supported in part by a Grant-in-Aid for Scientific Research (No. 63 550 630) from the Ministry of Science, Culture and Education of Japan, which is gratefully acknowledged.

(49) Sauer I.; Grezzo, L. A.; Staley, S. W.; Moore, J. H. *J. Am. Chem. Soc.* 1976, 98, 4218.

## Study of Cu(II) Binding to Chiral Tripodal Ligands by Electron Spin Echo Spectroscopy

Daniella Goldfarb,<sup>\*,†</sup> Jean-Michel Fauth,<sup>†</sup> Yitzhak Tor,<sup>‡</sup> and Abraham Shanzer<sup>†</sup>

Contribution from the Departments of Isotope Research and Organic Chemistry, The Weizmann Institute of Science, 76 100 Rehovot, Israel. Received May 16, 1990

**Abstract:** In an attempt to provide models for copper binding in proteins, symmetric and nonsymmetric chiral ligands designed to bind copper in a controlled geometry were synthesized. These ligands are assembled from trifunctional anchors extended by donors containing amino acids such as histidine and methionine. The copper coordination of these complexes was studied by orientation selective electron spin echo envelope modulation (ESEEM) experiments. The three-pulse FT-ESEEM spectra consist of peaks at 0.7, 1.4, 2.1, and 3.0 MHz, which positions are practically independent on the resonant magnetic field, and a peak at about 4 MHz, which shows significant field dependence. The relative intensities of all lines vary with the resonant field. These lines are typical for the remote nitrogen in the imidazole ring. By using computer simulations of the FT-ESEEM spectra recorded at the various resonant magnetic fields along the powder pattern and taking into account the selected excited orientations, the <sup>14</sup>N isotropic and anisotropic hyperfine interactions were determined. The simulations also gave the relative orientation of the <sup>14</sup>N hyperfine and quadrupole tensor principal axes with respect to the g tensor principal axis. From these parameters it was concluded that in the complexes consisting of three histidyl residues all three imidazoles are coordinated to the copper, not in a coplanar structure but in a propeller-like arrangement. No other nitrogens, such as the pivotal nitrogen, were found to be coordinated to the copper.

### Introduction

Copper ions are found in the active sites of a number of important proteins and enzymes of vital biological functions.<sup>1a-f</sup> These proteins are associated with a variety of processes including oxygen transport, electron transfer, superoxide dismutation, hydrolytic reactions, and many more. Crystallographic and spectral studies of many copper-containing metalloproteins have unraveled the nature of the metallic binding sites. In many cases they were found to be rather simple and composed of three amino acids which are invariable throughout the catalytic process. Histidine imidazoles frequently occupy one or more of the coordination sites, together with cysteine and methionine sulfur donors, and less frequently aspartic acid and glutamic acid carboxylates. Extensive research efforts have been devoted to model the active sites of these proteins with simple, low molecular weight compounds that would simulate the coordinative environments present in the natural systems.<sup>1b,g,h</sup>

We have recently introduced novel families of chiral tripod-like ligands,<sup>2</sup> where the attachment of a bidentate ligand to each one of the tripodal arms affords octahedral biomimetic metal binders. The tripodal approach is eminently suited for modelling also tetrahedral and lower symmetry coordination sites. By attaching a monodentate ligand to each tripodal arm the invariable part of three essential donors is generated. In this article we present a novel type of symmetrical and nonsymmetrical tripodal ligands which possess the naturally occurring amino acids. These ligands

are constructed from trifunctional anchors which are extended by donor containing chiral amino acids (e.g. histidine, methionine).

The extent of similarity between the synthetic models and natural proteins can be evaluated by comparing their spectral properties like ESR and electron spin echo envelope modulation (ESEEM) spectra.<sup>3</sup> ESEEM is particularly sensitive to the Cu(II) immediate environment since weak hyperfine interactions, normally hidden within the broad ESR line width, are easily detected. We thereby carried out a series of ESEEM experiments on the novel, tripodal ligand Tr(His)<sub>3</sub> (1) and its analogues, Ar(His)<sub>3</sub>

(1) (a) Siegel H., Ed. *Metal Ions in Biological Systems*; Dekker: New York, 1981; Vol. 13, Copper Proteins. (b) Solomon E. I. In *Copper Coordination Chemistry: Biochemical and Inorganic Perspectives*; Karlin, K. D., Zubieta, J., Eds.; Adenine Press: New York, 1983; pp 1–22. (c) Solomon, E. I.; Penfield, K. W.; Wilcox, D. E. *Struct. Bonding* 1983, 53, 1–57. (d) Reinhammar, B. *Adv. Inorg. Biochem.* 1979, 1, 91–118. (e) Beinert, H. *Coord. Chem. Rev.* 1980, 33, 55–85. (f) Fee, J. A. *Struct. Bonding* 1975, 23, 1–60. (g) Zubieta, J.; Karlin, K. D.; Hayes, J. C. In *Copper Coordination Chemistry: Biochemical and Inorganic Perspectives*; Karlin, K. D., Zubieta, J., Eds.; Adenine Press: New York, 1983; pp 97–108. (h) Urbach, F. L. *Metal Ions in Biological Systems*; Dekker: New York, 1981; Vol. 13, pp 73–115. (i) Sorrell, T. N. *Tetrahedron* 1989, 45, 3–68.

(2) (a) Tor, Y.; Libman, J.; Shanzer, A.; Lifson, S. *J. Am. Chem. Soc.* 1987, 109, 6517–6518. (b) Tor, Y.; Libman, J.; Shanzer, A. *J. Am. Chem. Soc.* 1987, 109, 6518–6519. (c) Libman, J.; Tor, Y.; Shanzer, A. *J. Am. Chem. Soc.* 1987, 109, 5880–5881. (d) Tor, Y.; Shanzer, A.; Scherz, A. *Inorg. Chem.* In press.

(3) Abbreviations used in the text; ESEEM, electron spin echo envelope modulation; NQR, nuclear quadrupole resonance; ENDOR, electron nuclear double resonance; LPSVD, linear prediction, singular value decomposition; Boc, *tert*-butoxycarbonyl; Tren, tris(2-aminoethyl)amine; CD, circular dichroism.

<sup>†</sup> Department of Isotope Research.

<sup>‡</sup> Department of Organic Chemistry.